

DIPSI: a Monte Carlo generator for elastic vector meson production in charged lepton-proton scattering

M. Arneodo^a, L. Lamberti^b and M. Ryskin^c

^a Università di Torino, via Giuria, 1, I-10125 Torino, Italy and
Università della Calabria and INFN, I-87036 Arcavacata di Rende (Cs), Italy
ARNEODO@VXDESY.DESY.DE

^b Università di Torino and INFN, via Giuria, 1, I-10125 Torino, Italy,
now at Imperial College, Blackett Laboratory, Prince Consort Rd., London SW7 2BZ, United Kingdom
LAMBL@VXDESY.DESY.DE

^c Petersburg Nuclear Physics Institute, 188350 Gatchina, Russia
RYSKIN@THD.PNPI.SPB.RU

Abstract

We present a Monte Carlo generator for exclusive vector meson production in charged lepton-proton interactions, $l + p \rightarrow l + p + V$, based on a QCD leading logarithm model calculation according to which the cross section for this process is proportional to the square of the gluon momentum density in the proton. The generator can be used for both fixed target and collider kinematics. Each event is assigned a weight equal to its cross section, so that the independent variables can be generated according to convenient distributions, not necessarily identical to the physics ones.

1 Introduction

In this paper we present a Monte Carlo generator for exclusive production of vector mesons in the reaction

$$e(\mu) + p \rightarrow e(\mu) + p + V, \quad (1)$$

where an electron (e) or a muon (μ) interacts with a proton (p), producing, in the final state, a vector meson V (ρ^0 , ω , ϕ , J/ψ ...). This reaction is also referred to as elastic vector meson production.

Figure 1 shows the diagram of the process; tables 1 and 2 define the relevant kinematic variables. The incoming lepton radiates a virtual photon of mass $-Q^2$ that collides with the target proton, turning into a vector meson; the proton emerges intact from the interaction. Since the vector meson has the same quantum numbers as the photon, the object exchanged between the photon and the proton, a pomeron, carries the quantum numbers of the vacuum.

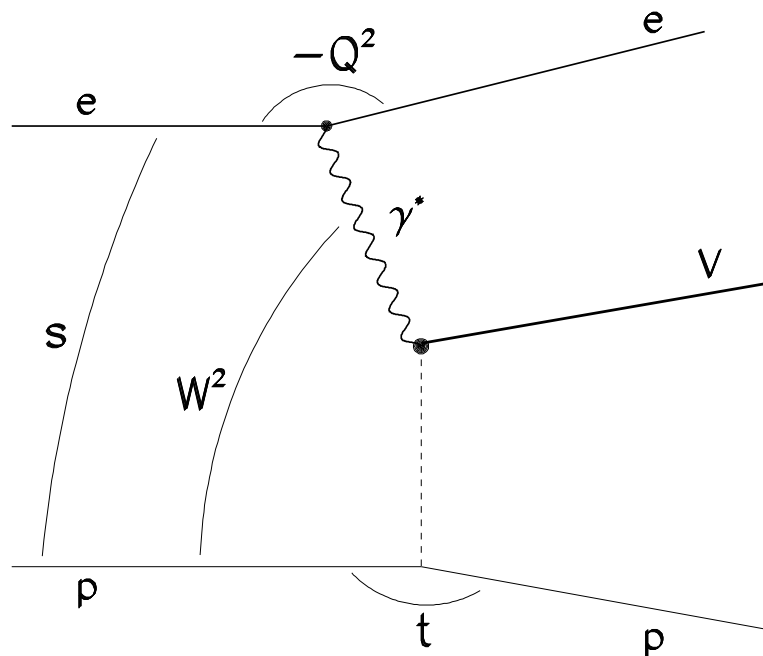


Figure 1: Elastic vector meson production.

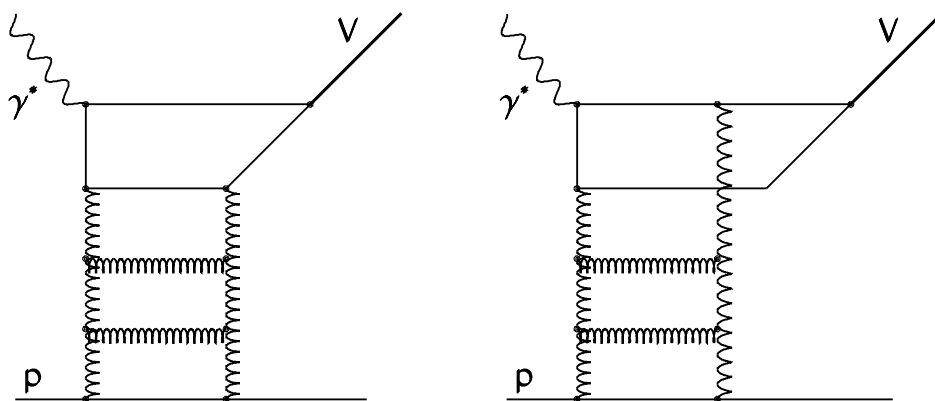


Figure 2: Elastic vector meson production in LLA.

k	four-momentum of the incident lepton
k'	four-momentum of the scattered lepton
p	four-momentum of the incident/target proton
p'	four-momentum of the scattered proton
v	four-momentum of the produced vector meson
m_V	mass of the vector meson
m_p	mass of the target proton
$q = k - k'$	four-momentum of the virtual photon
$-Q^2 = q^2$	invariant mass squared of the virtual photon
$y = p \cdot q / p \cdot k$	fraction of the beam energy carried by the photon (in the proton rest frame)
$\nu = p \cdot q / m_p$	photon energy (in the proton rest frame)
$W = \sqrt{(q + p)^2}$	photon-proton centre of mass energy
$\sqrt{s} = \sqrt{(k + p)^2}$	electron-proton centre of mass energy

Table 1: Definition of the relevant kinematic variables, part 1.

$t = (p - p')^2$	four-momentum squared exchanged at the proton vertex
p_t	transverse momentum of the vector meson with respect to the virtual photon direction
$z = p \cdot v / p \cdot q$	fraction of the photon energy carried by the vector meson (in the proton rest frame)
$x_t = \mathbf{p}' / \mathbf{p} $	ratio between outgoing and incoming proton three-momenta in the laboratory frame
p_t^P	transverse momentum of the proton in laboratory frame
$\bar{x} = \frac{Q^2 + m_V^2 + p_t^2}{W^2}$	fraction of the proton's momentum carried by the two-gluon system in the model of ref. [21]
$\bar{q}^2 = \frac{Q^2 + m_V^2 + p_t^2}{4}$	scale at which the gluon density is probed in the model of ref. [21]
ϑ	polar angle of the positive decay particle (e.g. π^+ in the ρ^0 case) with respect to the outgoing p direction in the V rest frame (for two-body decays)
φ	angle between the decay plane and the meson production plane, which contains the virtual photon and the meson, in the V rest frame (for two-body decays)
Φ	angle between the lepton scattering plane and the vector meson production plane (in the proton rest frame)
$\psi = \varphi - \Phi$	

Table 2: Definition of the relevant kinematic variables, part 2.

Pomerons were originally introduced to describe diffractive interactions between hadrons. Elastic vector meson production at small Q^2 can indeed be thought of as a hadronic process in the Vector Meson Dominance (VMD) [1] framework, in which the photon is assumed to fluctuate into a vector meson before interacting with the proton. Reaction (1) may thus allow the investigation of the properties of the pomeron, as well as of the hadronic features of the photon.

Elastic vector meson production has been extensively studied in fixed target experiments in the photoproduction regime ($Q^2 = 0$) [2]-[4] and at larger values of Q^2 [5]-[9], for photon-proton centre of mass energies $W \lesssim 20$ GeV. With the advent of the electron-proton collider HERA, reaction (1) has also been investigated at values of $W \approx 100$ GeV, both for $Q^2 \approx 0$ [10]-[15] and for non-zero virtualities [16]-[18].

From the theoretical point of view, several models [19]-[24] offer a description of elastic vector meson production; all assume pomeron exchange, with the pomeron described as a gluon pair. Individual models differ in the way the gluons are treated, ranging from non-perturbative approaches to perturbative ones.

The generator we wrote, hereafter referred to as DIPSI, is based on the model of ref. [21]¹. This model assumes that the exchanged virtual photon fluctuates into a $q\bar{q}$ pair which then interacts with a gluon ladder emitted by the incident proton (fig. 2). The parameters of the model are the strong coupling constant α_s , the two-gluon form factor of the proton and the gluon momentum density in the proton. Once these are chosen, the dependences on W and t , where t is the four-momentum squared transferred at the proton vertex, are fixed.

DIPSI has been extensively used within the ZEUS experiment – operating at the electron-proton collider HERA at DESY – in particular for the determination of the detector acceptance for ρ^0 [10, 11], ϕ [13] and J/ψ photoproduction [15] as well as for ρ^0 [16] and ϕ [18] production at large Q^2 .

The paper is organised as follows. In section 2 we give a short description of the model and in section 3 we present the program itself. The appendices contain a list of the files provided, a description of the input control cards as well as a list of the routines and functions used in the program.

2 The model

The model [21] is based on a perturbative QCD (pQCD) calculation of the $\gamma \rightarrow V$ process and assumes a non-relativistic wavefunction for the vector meson V . In the Born approximation, at small values of the parton fractional momentum x , the amplitude for the reaction $\gamma p \rightarrow Vp$ is given by the sum of those of the graphs shown in fig. 2 (without the “horizontal” gluons which form the rungs of the ladder), where the two t -channel gluons play the role of the pomeron (in the Born Low-Nussinov approximation [25]). It is convenient to write the contribution of the upper quark loop in terms of the electronic width $\Gamma_{\ell\ell}^V = \Gamma$ of the vector meson. In this way a large part of the $O(\alpha_s)$ corrections is absorbed in the experimental value of Γ ; here α_s is the strong coupling constant. To take into account logarithmic corrections which contain $(\alpha_s \ln q^2)^n$

¹The results of ref. [23] lead to formulae with the same structure.

or $(\alpha_s \ln 1/x)^m$ terms (here q^2 denotes the scale relevant for the process), one has to sum up a set of more complicated Feynman diagrams. In the axial gauge, these diagrams have the ladder form (i.e. include all gluons shown in fig. 2). At small t the lower part (that below the fermion loop) of the graphs of fig. 2 may be considered as the gluon momentum density in the proton $xg(x, q^2)$. Indeed, for $t = 0$ this lower part of the graph contains exactly the same Feynman diagrams (calculated for the same kinematics) as those involved in the definition of $xg(x, q^2)$ in the Leading Logarithm Approximation (LLA) QCD treatment of deep inelastic scattering.

The arguments x and q^2 of $xg(x, q^2)$ take the values $\bar{x} = (Q^2 + m_V^2 + p_t^2)/W^2$ and $\bar{q}^2 = (Q^2 + m_V^2 + p_t^2)/4$, respectively. The value of \bar{x} is larger than that of the Bjorken variable $x_{Bj} \simeq Q^2/W^2$, as one has to transfer additional longitudinal momentum along the pomeron (i.e. the t -channel gluons) to put the vector meson on mass shell.

The typical virtuality \bar{q} was chosen equal to $\frac{1}{2}\sqrt{Q^2 + m_V^2 + p_t^2}$ as the t -channel gluons interact with one quark only, which, in the non-relativistic approximation used in the model, carries one half of the external momenta (i.e. those of the photon and of vector meson).

At large energy the value of \bar{x} is small and for zero angle production, when $t = t_{\min} \simeq -\bar{x}^2 m_N^2 \rightarrow 0$, we can write the cross section in terms of Γ and $g(\bar{x}, \bar{q}^2)$. An explicit calculation gives:

$$\frac{d\sigma^T(\gamma p \rightarrow V p)}{dt} = \frac{\alpha_s^2(\bar{q}^2)\Gamma m_V^3}{3\alpha} \pi^3 \times \left[\bar{x}g(\bar{x}, \bar{q}^2) \frac{f(\bar{q}^2, p_t^2)}{2\bar{q}^2(2\bar{q}^2 - p_t^2) \ln(8\bar{q}^2/p_0^2)} \right]^2 [F_N^{2G}(t)]^2 \eta^2, \quad (2)$$

where $\alpha = 1/137$ is the electromagnetic coupling constant and the function $f(\bar{q}^2, p_t^2)$ is defined as follows:

$$f(\bar{q}^2, p_t^2) = \ln \left[\frac{4\bar{q}^2 - p_t^2 + p_0^2}{p_t^2 + p_0^2} \right] \text{ for } p_t^2 \leq p_0^2, \quad (3)$$

$$f(\bar{q}^2, p_t^2) = \ln \left[\frac{p_t^2 + p_0^2}{4\bar{q}^2 - p_t^2 + p_0^2} \frac{4\bar{q}^4}{p_t^4} \right] \text{ for } p_t^2 > p_0^2, \quad (4)$$

with the infrared cutoff parameter $p_0^2 = 0.5 \text{ GeV}^2$.

Part of the t (i.e. p_t^2) dependence of the amplitude is given by the bottom part of the graphs of fig. 2, i.e. by the spatial distribution of the colour charge inside the proton. We parametrise this distribution by means of the two-gluon form factor $F_N^{2G}(t)$ (with $F_N^{2G}(0) = 1$). This form factor cannot be calculated within pQCD and should be measured experimentally. The simplest hypothesis is that the function $F_N^{2G}(t)$ is close to the electromagnetic form factor and can thus be written, for instance, as $[F_N^{2G}(t)]^2 = e^{Bt}$, with $B \approx 5 \text{ GeV}^{-2}$ ²; equivalently the dipole approximation can be used. This hypothesis is implemented in the program. Unfortunately, within the LLA there is no shrinkage of the diffractive cone. Therefore the slope B does not

²However estimates based upon QCD sum rules [26] give somewhat smaller values of B .

depend on energy. This is a shortcoming of the model, and to imitate the effect of the diffractive cone shrinkage one should choose different values of B for different energies.

The remaining part of the t -dependence is contained in the factor $\{f/[\bar{q}^2(2\bar{q}^2-p_t^2)\ln(8\bar{q}^2/p_0^2)]\}^2$, which comes from the upper fermion loop in fig. 2, as well as in the \bar{x} and \bar{q}^2 dependence of the gluon distribution.

As mentioned above, a non-relativistic meson wavefunction is assumed. It is possible however to allow for relativistic effects by shifting the overall normalisation by a factor η^2 . For ρ^0 mesons $\eta \simeq 1.8$ [27], while it is expected to be close to unity for J/ψ mesons.

There are a few restrictions on the applicability of the model. In the first place, to be sure that $|t_{\min}| < \Lambda_{QCD}^2$ (or $|t_{\min}| < 1/R_N^2$, with R_N the nucleon radius), only the region $\bar{x} < 0.1$ should be considered.

Furthermore, strictly speaking, one should use the pQCD result only at sufficiently large values of \bar{q}^2 , say $\bar{q}^2 > 2 \text{ GeV}^2$. Nevertheless, the program can be used also at smaller values of \bar{q}^2 , e.g. for ρ^0 photoproduction, for which $\bar{q}^2 \simeq 0.15 \text{ GeV}^2$. This is the reason for modifying formula (6) of ref. [21] into (2) by including an infrared cutoff. There are no singularities for $\bar{q}^2 > \Lambda_{QCD}^2$; however the applicability of pQCD for these values of \bar{q}^2 is questionable. Parametrisations can be found for $\bar{x}g(\bar{x}, \bar{q}^2)$, with which the experimental results on ρ^0 photoproduction are reproduced [10, 11]; in this region however it is not clear whether the function $\bar{x}g(\bar{x}, \bar{q}^2)$ can still be interpreted as the gluon momentum density in the proton.

We have so far discussed only the case of transversely polarised photons. The exchange of a pQCD (two-gluon) pomeron conserves s -channel helicity³ and, if the vector meson wavefunction has the non-relativistic form, the longitudinal cross section is given by $\sigma^L = (Q^2/m_V^2)\sigma^T$. In the program both the σ^L and σ^T terms are taken into account with the corresponding angular distributions for the vector meson decay products. As an example, in the case of two-body decays, the cross section is written as:

$$\frac{d^2\sigma^T}{d\cos\vartheta d\bar{\psi}} = \frac{1}{4\pi}\sigma^T k_T(\cos\vartheta, \bar{\psi}), \quad (5)$$

$$\frac{d^2\sigma^L}{d\cos\vartheta d\bar{\psi}} = \frac{1}{4\pi}\sigma^L k_L(\cos\vartheta, \bar{\psi}), \quad (6)$$

where ϑ and ψ are defined in table 2 and $\bar{\psi} = \psi + \delta$, with δ the angle that the photon polarisation vector forms with the normal to lepton scattering plane; this angle is taken to be zero with probability $(2-y)^2/Ny^2$ and 90° with probability $1/N$, where $N = 1 + (2-y)^2/y^2$.

The angle ψ is the difference of the azimuthal angles φ and Φ , which are defined in two different frames. These frames however differ by a boost which is very nearly (to an accuracy better than $(Q^2 + p_t^2)/s$) perpendicular to the quantisation axes of both frames, thus hardly affecting the azimuthal distributions.

For decays to spin-1/2 particles (e.g. $J/\psi \rightarrow e^+e^-$), one has $k_T(\cos\vartheta, \bar{\psi}) = 3/2(1 - \sin^2\vartheta \cos^2\bar{\psi})$ and $k_L(\cos\vartheta) = 3/2 \sin^2\vartheta$. For decays to spin-0 particles (e.g. $\rho^0 \rightarrow \pi^+\pi^-$),

³There was a mistake in sect. 3 of ref. [21], where the helicity flip amplitude $A_{1,0}$ was indicated to be non-zero. One of us (M.R.) would like to thank D. Krücker for pointing this out.

the angular distributions become $k_T(\cos \vartheta, \bar{\psi}) = 3 \sin^2 \vartheta \cos^2 \bar{\psi}$ and $k_L(\cos \vartheta) = 3(1 - \sin^2 \vartheta)$, respectively.

In the case of the three-body decay $V \rightarrow \pi^+ \pi^- \pi^0$, the angular distributions are given by $k_T(\cos \vartheta, \bar{\psi}) \propto \sin^2 \vartheta \cos^2 \bar{\psi}$ and $k_L(\cos \vartheta) \propto (1 - \sin^2 \vartheta)$, where now ϑ and $\bar{\psi}$ are defined as in the two-body decay case but for the normal to the decay plane rather than for the π^+ direction.

For all other decay modes, the function k is taken as constant.

The γp cross section is related to the ep (or μp) cross section as follows:

$$\frac{d^2\sigma(ep \rightarrow epV)}{dydQ^2} = \Gamma_T \sigma^T(\gamma p \rightarrow Vp) + \Gamma_L \sigma^L(\gamma p \rightarrow Vp), \quad (7)$$

where Γ_T and Γ_L are the fluxes of transversely and longitudinally polarised virtual photons, respectively. Their explicit expression is:

$$\Gamma_T = \frac{\alpha}{2\pi Q^2} \left[\frac{1 + (1-y)^2}{y} - \frac{2(1-y)}{y} \frac{Q_{\min}^2}{Q^2} \right], \quad (8)$$

$$\Gamma_L = \frac{\alpha}{2\pi Q^2} \frac{2(1-y)}{y}, \quad (9)$$

where $Q_{\min}^2 = M_e^2 \frac{y^2}{1-y}$ is the minimum value of Q^2 kinematically allowed.

3 The program

DIPSI generates events according to reaction (1) in which V can be, at present:

- $\rho^0 \rightarrow \pi^+ \pi^-$,
- $\omega \rightarrow \pi^+ \pi^- \pi^0$ or $\pi^+ \pi^-$,
- $\phi \rightarrow K^+ K^-$, $K_L^0 K_S^0$ or $\pi^+ \pi^- \pi^0$,
- $\rho(1450) \rightarrow \pi^+ \pi^-$, $\pi^+ \pi^- \rho^0$ or $\pi^0 \pi^0 \rho^0$,
- $\rho(1700) \rightarrow \pi^+ \pi^-$, $\pi^+ \pi^- \rho^0$ or $\pi^0 \pi^0 \rho^0$,
- $J/\psi \rightarrow e^+ e^-$, $\mu^+ \mu^-$ or $\pi^+ \pi^- \pi^0$,
- $\psi'(3600) \rightarrow e^+ e^-$, $\mu^+ \mu^-$, $\pi^+ \pi^- J/\psi$ or $\pi^0 \pi^0 J/\psi$,
- $\Upsilon \rightarrow e^+ e^-$, $\mu^+ \mu^-$ or $\pi^+ \pi^- \pi^0$.

The program is steered by control cards, in which the user should fix, for each run, some parameters and choose among a few options:

- lepton beam type (electron, muon);
- beam momenta (for fixed target kinematics the proton beam momentum has to be set to 0; the lepton beam momentum must always be negative);
- generation limits for Q^2 , y and p_t^2 and type of generation for each of these variables (as described in section 3.1);
- type of meson produced, decay mode and mass spectrum;
- value of α_s , gluon density and proton form factor;
- amount of output data.

Before discussing the structure of the program and its features, we describe the method of weighted events on which the generator is based.

3.1 The method of weighted events

Each event generated with DIPSI is assigned a weight equal to its cross section. This makes it possible to decouple the generation of the independent variables from their expected distribution.

As an example, let us consider the p_t^2 distribution. The model predicts an approximately exponential distribution of the type $A \exp(-bp_t^2)$; suppose that for a given vector meson $b = 10 \text{ GeV}^{-2}$. If events are generated according to such a distribution it may take considerable computer time to substantially populate the high p_t^2 region. In order to study the high p_t^2 tail, one can instead choose to generate with, say, $b = 3 \text{ GeV}^{-2}$. To obtain a physically meaningful p_t^2 distribution one has then to weight each event with its cross section and with a factor, that we will name “phase space factor”, which takes into account the way in which the variable has been generated.

Assume, for the sake of simplicity, that the model had only one independent variable, ξ . Suppose that, given a random number R_i between zero and unity, sampled from a uniform distribution, one obtains a value ξ_i for ξ using some algorithm $\xi = \xi(R)$ which is able to populate adequately the region of ξ under study. Based on the model, the value of $d\sigma/d\xi_i$, the differential cross section $d\sigma/d\xi$ for $\xi = \xi_i$, can then be computed. The weight of the event is given by

$$\sigma_i = \frac{d\sigma}{d\xi_i} \frac{d\xi}{dR_i}, \quad (10)$$

where the phase space factor $d\xi/dR_i$ is the value of $d\xi/dR$ computed for $R = R_i$. The phase space factor would be unity if ξ were sampled from a uniform distribution in the range 0-1.

The cross section for the process, integrated over the generation range of ξ , is thus

$$\sigma = \frac{1}{N_{tot}} \sum_{i=1}^{N_{tot}} \sigma_i, \quad (11)$$

where N_{tot} is the total number of generated events. The statistical uncertainty on σ is given by

$$\Delta\sigma = \frac{1}{N_{tot}} \sqrt{\sum_{i=1}^{N_{tot}} \sigma_i^2}. \quad (12)$$

Likewise, the differential cross section $d\sigma/d\xi$ for $\xi = \xi_i$ is obtained as

$$\frac{d\sigma}{d\xi} = \frac{1}{\Delta\xi} \sum_{bin} \sigma_i / N_{tot} = \frac{1}{\Delta\xi N_{tot}} \sum_{bin} \sigma_i, \quad (13)$$

where the sum is extended to the events in a narrow bin of width $\Delta\xi$ centred around ξ_i .

3.2 The structure of the program

The code consists of three main routines: DIPSINI, which controls the initialisation phase; DIPSIGEN, for the actual event generation; DIPSOUT, which terminates the program.

3.2.1 Initialisation

In DIPSINI the relevant variables are initialised, the random number seed and the external input cards are read in and the histograms and n-tuples are booked. The input quantities read from the control cards are described in appendix C.

3.2.2 Event generation

For each event the following independent kinematic variables are generated (subroutine DIPSIGEN): y , Q^2 , the mass of the vector meson m_V , p_t^2 and the azimuthal angles of the scattered lepton with respect to the incoming beam direction and of the vector meson with respect to the virtual photon direction. The four-momenta of the scattered lepton, of the vector meson and of the scattered proton are then fixed by energy-momentum conservation.

Various options, detailed in appendix C, are available for generating y (flat, $1/y$), Q^2 (flat, $1/Q^2$, $1/Q^4$) and m_V (flat, Breit-Wigner, Söding [28, 10], relativistic p-wave Breit-Wigner). The variable p_t^2 is sampled from an exponential distribution of which the user can choose the slope.

Once the kinematics of the event has been generated, the cross section is evaluated as discussed in sect. 2 by subroutine JPRYSKIN, called by DIPSIGEN. Immediately after calling JPRYSKIN, DIPSIGEN evaluates the weight by multiplying the cross section by the phase space factors. In addition to the weight for the process $ep \rightarrow epV$, that for the reaction $\gamma^*p \rightarrow Vp$ is also computed.

Finally subroutines JDK (for two-body decays) and TREDK (for three-body decays), also called by DIPSIGEN, let the vector meson decay. At this point the weight is modified so as to take into account the dependence of the cross section on the decay angular variables; these variables are evaluated by the routines DPHELI and HELOMEGA for two-body and three-body decays, respectively.

3.2.3 Termination

Subroutine DIPSOUT computes the integrated ep and γ^*p cross sections according to expression (11) and closes histogram and n-tuple files.

3.3 Implementation and usage

DIPSI is written in standard FORTRAN 77 and uses the PATCHY offline editor [29] to allow easier modifications. All routines are contained in a PAMfile; a short “cradle” program contains the list of the routines that the user wants to include and the modifications to the code, if any, that need to be applied. By running PATCHY on the PAMfile a FORTRAN program is produced.

The CERN libraries PACKLIB and KERNLIB [30] are necessary; extensive use is made of the format free reading package FFREAD [31] and of the histogramming package HBOOK [32] (which is a part of PACKLIB). The parton distribution package PDFLIB [33] may be needed (cf. appendix B.1).

3.3.1 Input

All necessary input parameters are read in from the user control cards (logical unit 8) described in appendices B and C. A second input file (logical unit 9) is used in order to keep track of the random number seeds. These are the only input files.

Among the input quantities are the gluon distribution, the strong coupling constant and the proton form factor. Concerning these parameters a remark is in order. The cross section factorises in α_s^2 , in the gluon density squared and in the proton form factor squared. It is thus not necessary to generate new samples of events if one exists already and if any of these quantities is modified: it is sufficient to reweight the events. As an example, if events have been generated with a gluon density $\bar{x}g(\bar{x}) = 3(1 - \bar{x})^5$ and one wants to change to a different distribution $\bar{x}g'(\bar{x}, \bar{q}^2)$, the weight of each event should be multiplied by the factor $[(\bar{x}g')/(\bar{x}g)]^2$. If desired, however, a user provided parametrisation can be included in subroutine USRGLS; in that case the switch USRGLU in the control cards should be set to 1. The default version of the subroutine contains, as an example, a call to the MRSA parametrisation from the library PDFLIB [33]; the user can replace it with any other.

3.3.2 Output

DIPSI produces the following output files:

1. DIPSI.TST (logical unit 18), a log-file listing the values of the input parameters selected via the control cards, the integrated ep (or μp) and the integrated γ^*p cross sections;
2. DIPSI.OUT (logical unit 6), containing the same log-file along with the HBOOK histograms in ASCII format;

EBEAM	-27.5	JDKLEP	2
PBEAM	820.00	IMASGE	0
NTPFLAG	1	MASMIN	0.3
EMC	0	MASMAX	1.5
NUTO	300000	USRGLU	0
JEVE	0	ICRXGX	0
YMIN	1.E-2	IQ2EVO	0
YMAX	0.99	IFORFA	0
YGEN	0	FORFAS	2.5
QSQLOW	4.	BIPT	3.0
QSQUP	100.	PTMIN	0.0
KEWGEN	0	PTMAX	10.000
JMESON	1	ALPHAS	0.25
		ETA	1.

Table 3: Cards used to produce the sample of events with elastic production of ρ^0 mesons in the range $4 < Q^2 < 100 \text{ GeV}^2$ at HERA, cf. figs. 3 and 4. See appendix C for an explanation of the meaning of the cards.

3. DIPSI.HROUT (logical unit 40), with the same histograms readable with PAW [34];
4. DIPSI.NTP (logical unit 41), containing the n-tuple;
5. DIPSI.ERR (logical unit 19), containing (self-explanatory) error messages, if any;
6. DIPSI.UNO (logical unit 17), containing all kinematic variables and momenta for a single event. The event number is chosen via the card JEVE.

Figures 3 to 6 show some typical plots. Figures 3 and 4 show the Q^2 , y , W , t and decay angles distributions for a sample of ρ^0 mesons generated in the HERA kinematic regime, with $4 < Q^2 < 100 \text{ GeV}^2$ and $0.01 < y < 0.99$. Figures 5 and 6 show the same plots for a J/ψ sample produced in the photoproduction regime at HERA. For this sample $Q^2 < 4 \text{ GeV}^2$ and $0.01 < y < 0.99$. Tables 3 and 4 list the cards used to produce these samples (see appendix C for a description of the cards).

4 Summary

We presented a Monte Carlo generator for elastic vector meson production via reaction (1), based on a leading logarithm QCD model calculation [21].

The model parameters are the strong coupling constant, the two-gluon proton form factor and the gluon distribution in the proton. The cross section is proportional to the square of the gluon momentum distribution in the nucleon.

EBEAM	-27.5	JDKLEP	0
PBEAM	820.00	IMASGE	0
NTPFLAG	1	MASMIN	0
EMC	0	MASMAX	0
NUTO	100000	USRGLU	0
JEVE	0	ICRXGX	0
YMIN	1.E-2	IQ2EVO	0
YMAX	0.99	IFORFA	0
YGEN	0	FORFAS	2.50
QSLOW	1.E-12	BIPT	3.00
QSQUP	4.	PTMIN	0.000
KEWGEN	0	PTMAX	10.000
JMESON	0	ALPHAS	0.25
		ETA	1.

Table 4: Cards used to produce the sample of events with elastic photoproduction of J/ψ mesons at HERA, cf. figs. 5 and 6. See appendix C for an explanation of the meaning of the cards.

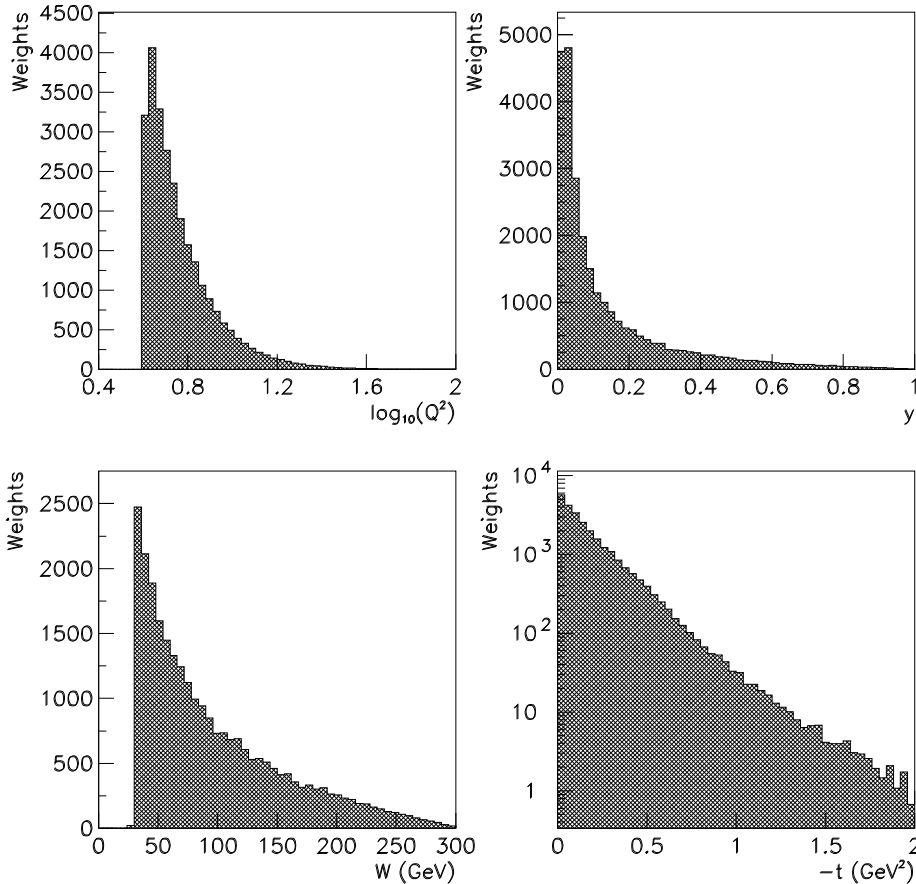


Figure 3: Distributions over Q^2 , y , W and t for events with elastic production of ρ^0 mesons in the range $4 < Q^2 < 100 \text{ GeV}^2$ at HERA. See table 3 for the list of the cards used.

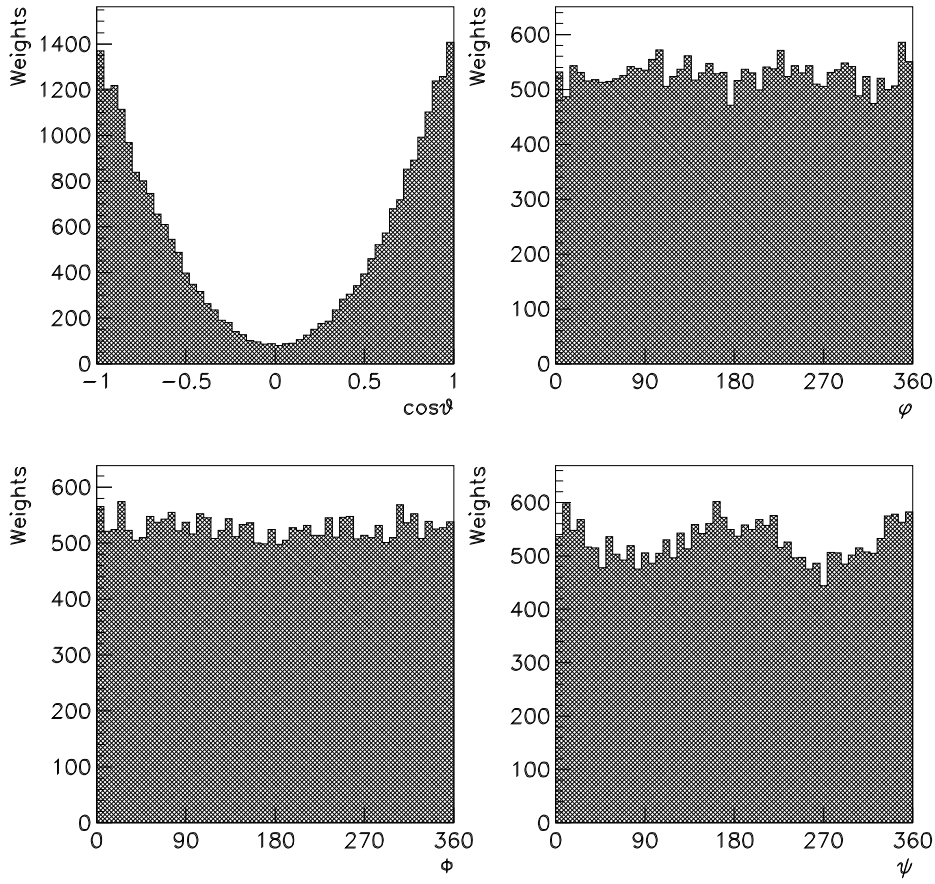


Figure 4: Distributions over $\cos\vartheta$, φ , Φ and ψ for events with elastic production of ρ^0 mesons in the range $4 < Q^2 < 100 \text{ GeV}^2$ at HERA. See table 3 for the list of the cards used.

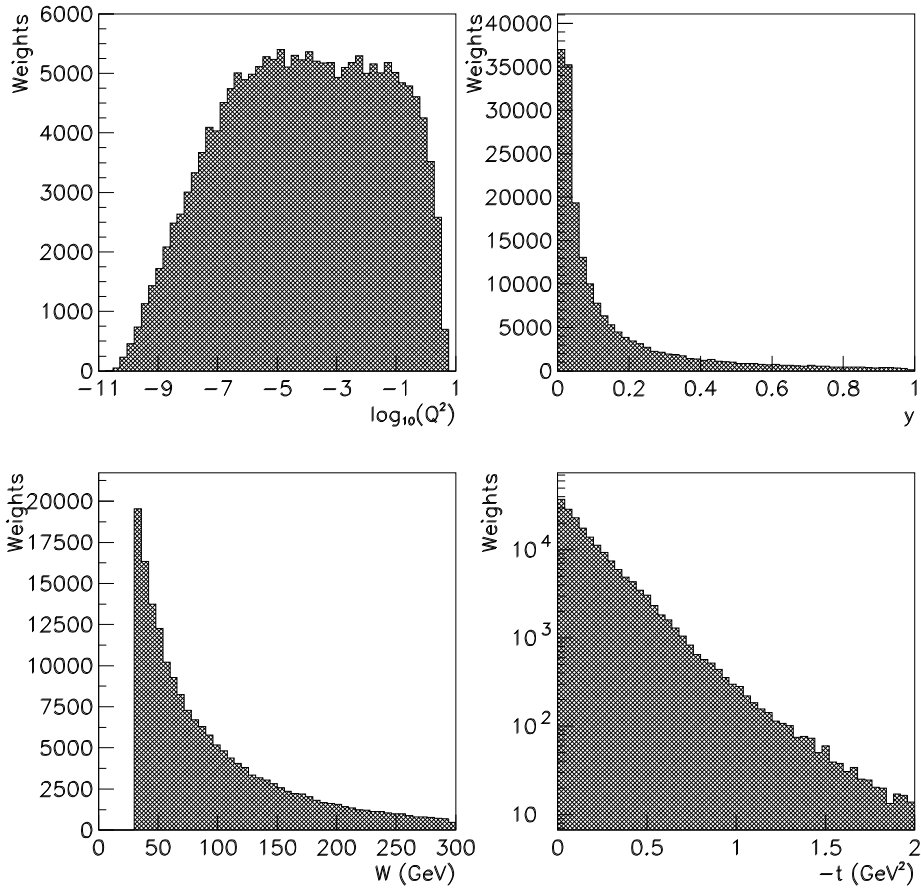


Figure 5: Distributions over Q^2 , y , W and t for events with elastic photoproduction of J/ψ mesons at HERA. See table 4 for the list of the cards used.

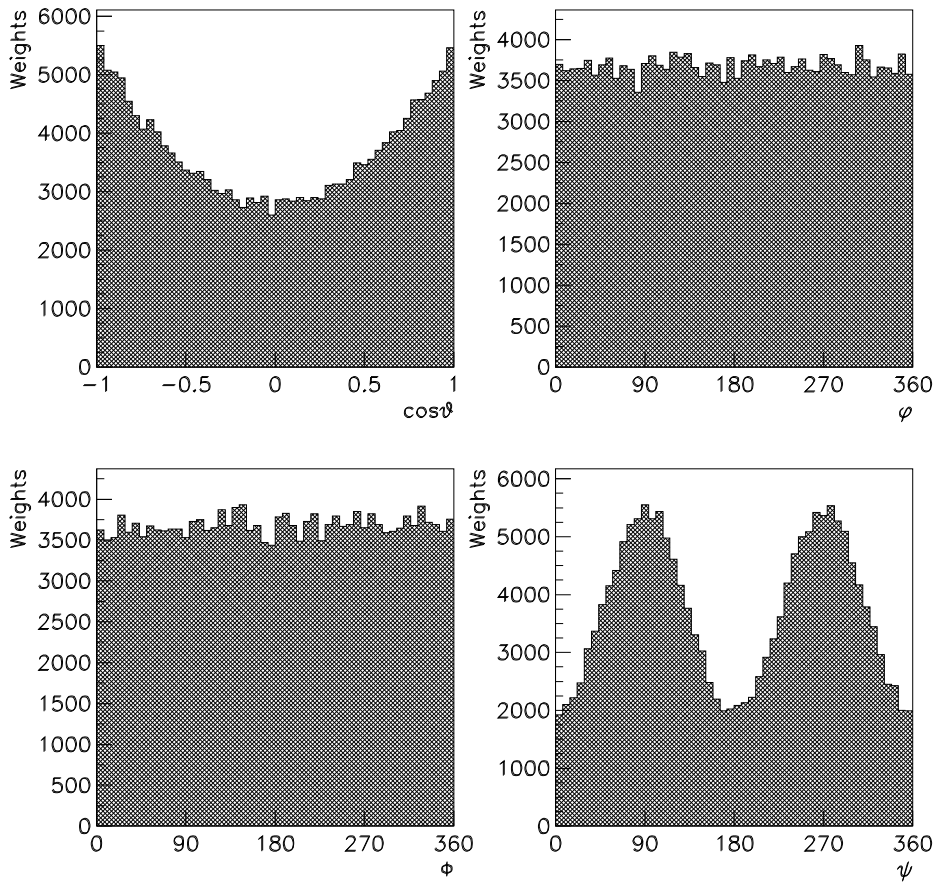


Figure 6: Distributions over $\cos\vartheta$, φ , Φ and ψ for events with elastic photoproduction of J/ψ mesons at HERA. See table 4 for the list of the cards used.

The program correctly describes the ZEUS data on photoproduction of ρ^0 [10, 11] and J/ψ mesons [15], and has been used to evaluate the ZEUS acceptance for these and other processes. It is interesting that, with suitable input for the gluon distribution, DIPSI reproduces also the ρ^0 photoproduction data, which are in a \bar{q}^2 region ($\bar{q}^2 \approx 0.15 \text{ GeV}^2$) below that of applicability of perturbative QCD.

DIPSI is steered by control cards by means of which the user can select, among other features, the type and decay mode of the vector meson, the kinematic regime, the range of the independent variables and the distribution from which they are sampled.

Each event is assigned a weight proportional to its cross section. It is thus possible to generate the independent variables according to distributions different from those expected by the model, thereby enhancing, if necessary, the statistical significance of the sample in regions where the cross section is small.

5 Acknowledgements

We are indebted to Cristiana Peroni who proposed that we write DIPSI. We are grateful to her and to Aldus Whitfield for a critical reading of the manuscript. We would also like to thank Alexander Proskuryakov, Andrzej Sandacz and Ada Solano for many useful discussions.

Some routines of DIPSI are based on similar ones belonging to generators for inelastic J/ψ production developed within the EMC and NMC collaborations at CERN; we are grateful to Terry Sloan, Maarten de Jong and Chiara Mariotti for many discussions on those programs and on the EMC and NMC J/ψ data.

Many thanks are also due to our ZEUS and NMC colleagues who have used DIPSI up to now, thus actively contributing to the debugging process.

Finally, one of us (M.R.) is grateful to INFN for financial support while in Italy.

A List of the files provided

The following files are provided:

```
DIPSI24.CAR
DIPSI.CRA
DIPSI.CARDS
DIPSI.COM
DIPSI.UNIX.
```

They are respectively the PATCHY pamfile (card version) and cradle, the control cards, and the command-files in VMS and in UNIX. The cradle file includes a PATCHY switch to be set depending on whether the program is run in a UNIX or a VMS environment.

B Selection of model parameters

B.1 The gluon momentum density

In order to compute the gluon distribution in the proton, two subroutines are provided, GLUONS and USRGLS.

In GLUONS a few distributions are implemented. The default one is $\bar{x}g(\bar{x}) = 3(1 - \bar{x})^5$; also available is the parametrisation obtained by the NMC experiment [35].

The card ICRXGX (cf. appendix C) selects the available parametrisations:

- ICRXGX=0: $\bar{x}g(\bar{x}) = 3(1 - \bar{x})^5$;
- ICRXGX=1: NMC lower limit for $\bar{q}^2 = 7 \text{ GeV}^2$;
- ICRXGX=2: NMC central value for $\bar{q}^2 = 7 \text{ GeV}^2$;
- ICRXGX=3: NMC upper limit for $\bar{q}^2 = 7 \text{ GeV}^2$.

Furthermore, if ICRXGX=2:

1. IQ2EVO=1: a \bar{q}^2 dependent parametrisation [36] of the NMC results is used (fig. 7);
2. IQ2EVO=2: same as IQ2EVO=1 but $\bar{x}g(\bar{x}, \bar{q}^2) = \bar{x}g(\bar{x}, \bar{q}_{\min}^2)$ for $\bar{q}^2 \leq \bar{q}_{\min}^2 = 2 \text{ GeV}^2$;
3. IQ2EVO=3: same as IQ2EVO=2 but $\bar{x}g(\bar{x}, \bar{q}^2) = \bar{x}_{\min}g(\bar{x}_{\min}, \bar{q}^2)$ for $\bar{x} \leq \bar{x}_{\min} = 3 \times 10^{-3}$.

The routine USRGLS is a dummy routine with arguments \bar{x} , \bar{q}^2 and $\bar{x}g$ which returns the value of $\bar{x}g(\bar{x}, \bar{q}^2)$ for the given \bar{x} and \bar{q}^2 . The user can implement the desired parametrisation here. The default version of the subroutine contains, as an example, a call to the MRSA parametrisation from the library PDFLIB [33].

Finally it is possible to switch from GLUONS to USRGLS by means of the integer card USRGLU: USRGLU = 1 allows the use of USRGLS (see appendix C).

B.2 The two-gluon form factor of the proton

The choice of the proton form factor can be done directly via cards (cf. appendix C). The card IFORFA allows to choose between the dipole form factor, $F_N(t) = 1/(1 - \frac{t}{0.71})^2$, (IFORFA=0) and an exponential one (IFORFA=1). In the latter case the slope of the exponential can be set via card FORFAS.

B.3 The strong coupling constant α_s

The value of the strong coupling constant α_s is determined by card ALPHAS (see appendix C). A card value in the range between 0 and 1 fixes α_s to the card value. ALPHAS values outside the range 0-1 let α_s evolve with \bar{q}^2 , assuming $\alpha_s(\bar{q}^2) = 12\pi/[25 \ln(\bar{q}^2/\Lambda_{QCD}^2)]$; in this case, if α_s comes out to be larger than 0.7, it is automatically set to 0.7. The value of Λ_{QCD} is set to 200 MeV.

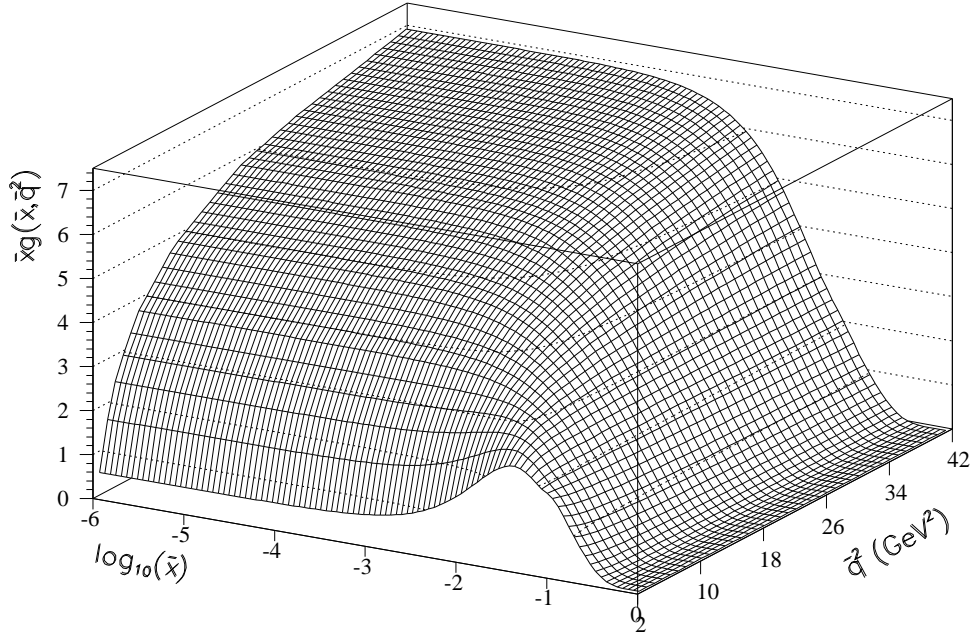


Figure 7: The gluon distribution in the proton as parametrised in [36].

B.4 Relativistic effects in the meson wavefunctions

It is possible to shift the normalisation of the cross section to account for relativistic effects in the meson wavefunctions. The cross section can be multiplied by a factor $[\eta^2]$; the user can choose it by setting the card ETA to the desired value. Zero or negative values are equivalent to setting $\eta = 1$. For the ρ^0 meson a value $\eta = 1.8$ is recommended [27]. For J/ψ mesons $\eta \approx 1$.

C Input control cards

An example of input control card file (logical unit 8), with a description of each entry, is given below. For more details on the cards controlling the gluon distribution, the form factor of the proton, α_s and η , see appendix B.

```

C *** Lepton beam momentum in GeV (must be negative...)
EBEAM      -27.5
C *** Proton beam momentum in GeV
PBEAM      820.00
C *** ntpflag = 0/1: do not fill/fill n-tuple
NTPFLAG    1
C *** emc = 0: electron beam, emc = 1: muon beam
EMC        0
C *** Total number of events to be generated
NUTO       11000
C *** Event to be dumped in dipsi.uno
JEVE       4
C *** y generation range and spectrum: YGEN = 0 --> 1/Y,

```

```

C ***                               YGEN = 1 --> flat
YMIN          4.E-2
YMAX          9.E-2
YGEN          1
C *** Q2 generation range (in GeV2) and spectrum:
C *** KEWGEN = 0 --> 1/Q2, KEWGEN = 1 --> 1/Q4, KEWGEN = 2 --> flat
QSLOW         .10E-9
QSUP          5.00E+0
KEWGEN        0
C *** JMESON: vector meson type
C           0 J/psi (also any integer other than the ones below)
C           1 rho
C           2 phi
C           3 Upsilon
C           4 omega
C           10 psi'(3686)
C           11 rho'(1450)
C           21 rho'(1700)
JMESON        0
C *** JDKLEP: decay mode
C           0 mu+ mu- (also any integer other than the ones below)
C           1 e+ e-
C           2 pi+ pi-
C           3 K+ K-
C           4 K0s K0L
C           5 pi+ pi- pi0 (with pi0 --> gamma gamma)
C           10 pi+ pi- psi --> pi+ pi- mu+ mu-
C           11 pi+ pi- psi --> pi+ pi- e+ e-
C           12 pi+ pi- rho --> pi+ pi- pi+ pi-
C           15 pi0 pi0 psi --> pi0 pi0 mu+ mu- (pi0s do not decay)
C           16 pi0 pi0 psi --> pi0 pi0 e+ e- (pi0s do not decay)
C           17 pi0 pi0 rho --> pi0 pi0 pi+ pi- (pi0s do not decay)
JDKLEP        1
C *** IMASGE: Vector meson mass distribution
C           0 Breit Wigner (also any integer other than the
C                   ones below)
C           1 flat
C           2 Soeding (cf. ref. [28] and [10])
C           3 relativistic p-wave BW
IMASGE        0
C *** MASS GENERATION RANGE
C
MASMIN        1.00
MASMAX        2.40
C *** Input gluon distribution (cf. appendix B.1)
USRGLU        0
ICRXGX        0

```

```

C *** Q2 evolution:      IQ2EVO=0 --> no q2 evolution,
C ***                    IQ2EVO=1 --> NMC xg(x,q2)
C *** (cf. appendix B.1)
IQ2EVO          0
C *** Proton form factor: IFORFA=0 --> dipole,
C ***                    IFORFA=1 --> exponential
C *** (cf. appendix B.2)
IFORFA          0
C *** Form factor slope (cf. appendix B.2)
FORFAS          2.50
C *** Pt2 (exponential) generation spectrum and range (in GeV2)
C *** BIPT = generation slope (in GeV-2)
PTMIN           0.000
PTMAX           1000.000
BIPT            5.00
C *** Alpha strong (cf. appendix B.3)
ALPHAS          0.25
C *** normalisation shift to account for
C *** relativistic wavefunction (cf. appendix B.4)
ETA             1.
C
STOP

```

D Contents of the n-tuple

Logical unit 41 is an unformatted file in which we store many of the relevant kinematic variables as an n-tuple. In the following we give a brief description of the contents of this n-tuple. For a definition of the symbols the reader is referred to tables 1 and 2. The n-tuple ID number is 666.

The components of particle momenta are given in the following order: x , y and z components of three-momentum, energy and mass. The z axis coincides with the incoming proton direction and is opposite to the direction of the incoming electron. If the proton is at rest the z axis is also taken to be opposite to the direction of the incoming electron. Energy, momenta and masses are expressed in GeV; cross sections are in nb. Lines from 56 to 70 are relevant only for three-body decays. For these decays ϑ and φ are the polar and azimuthal angles of the normal to the decay plane in the helicity frame. The term ‘unstable meson’ refers to π^0 , ρ^0 and J/ψ .

```

*****
* NTUPLE ID= 666 ENTRIES= 100000 DIFFRACTIVE JPSI EVENTS
*****
* Var numb * Name * Lower * Upper *
*****
* 1 * Q2 * 0.100249E-09 * 0.499924E+01 *  $Q^2$ 
* 2 * Y * 0.100000E-01 * 0.499995E+00 *  $y$ 
* 3 * NU * 0.480671E+03 * 0.240333E+05 *  $\nu$ 
* 4 * PT2CM * 0.194709E-05 * 0.466549E+01 *  $p_t^2$ 
* 5 * WSQ * 0.899670E+03 * 0.451005E+05 *  $W^2$ 

```

*	6	* Z	* 0.997422E+00	* 0.100000E+01	* z
*	7	* T	* -.600013E-03	* 0.467034E+01	* $-t$
*	8	* XL	* 0.979781E+00	* 0.999787E+00	* x_l
*	9	* PT	* 0.139538E-02	* 0.215999E+01	* p_t^p
*	10	* XBAR	* 0.212857E-03	* 0.168337E-01	* \bar{x}
*	11	* Q2BAR	* 0.239770E+01	* 0.423783E+01	* \bar{q}^2
*	12	* HCOSTH	* -.999990E+00	* 0.999992E+00	* $\cos \vartheta$
*	13	* HPHI	* 0.123719E-02	* 0.628306E+01	* φ
*	14	* HPHIC	* 0.184483E-02	* 0.628304E+01	* Φ
*	15	* HPSI	* 0.150895E-02	* 0.628255E+01	* ψ
*	16	* WEIGHT	* 0.897848E-05	* 0.546283E+01	* ep weight
*	17	* WTGAMP	* 0.565991E-04	* 0.263028E+02	* γp weight
*	18	* EBE1	* 0.000000E+00	* 0.000000E+00	* incoming
*	19	* EBE2	* 0.000000E+00	* 0.000000E+00	* lepton
*	20	* EBE3	* -.275000E+02	* -.275000E+02	*
*	21	* EBE4	* 0.275000E+02	* 0.275000E+02	*
*	22	* EBP1	* 0.000000E+00	* 0.000000E+00	* target
*	23	* EBP2	* 0.000000E+00	* 0.000000E+00	* proton
*	24	* EBP3	* 0.820000E+03	* 0.820000E+03	*
*	25	* EBP4	* 0.820001E+03	* 0.820001E+03	*
*	26	* ESE1	* -.221037E+01	* 0.219890E+01	* scattered
*	27	* ESE2	* -.220185E+01	* 0.219534E+01	* lepton
*	28	* ESE3	* -.272250E+02	* -.137196E+02	*
*	29	* ESE4	* 0.137501E+02	* 0.272669E+02	*
*	30	* ESE5	* 0.511000E-03	* 0.511000E-03	*
*	31	* ESP1	* -.179924E+01	* 0.161310E+01	* recoiling
*	32	* ESP2	* -.197851E+01	* 0.187068E+01	* proton
*	33	* ESP3	* 0.803420E+03	* 0.819825E+03	*
*	34	* ESP4	* 0.803421E+03	* 0.819826E+03	*
*	35	* ESP5	* 0.938272E+00	* 0.938272E+00	*
*	36	* GAM1	* -.219890E+01	* 0.221037E+01	* virtual
*	37	* GAM2	* -.219534E+01	* 0.220185E+01	* photon
*	38	* GAM3	* -.137804E+02	* -.275000E+00	*
*	39	* GAM4	* 0.233082E+00	* 0.137499E+02	*
*	40	* GAM5	* -.223590E+01	* 0.428417E-02	*
*	41	* VEC1	* -.306449E+01	* 0.294946E+01	* vector
*	42	* VEC2	* -.298695E+01	* 0.297885E+01	* meson
*	43	* VEC3	* -.135730E+02	* 0.162611E+02	*
*	44	* VEC4	* 0.309709E+01	* 0.168128E+02	*
*	45	* VEC5	* 0.309690E+01	* 0.309690E+01	*
*	46	* MUP1	* -.322182E+01	* 0.326902E+01	* first
*	47	* MUP2	* -.339305E+01	* 0.353246E+01	* decay
*	48	* MUP3	* -.136807E+02	* 0.127291E+02	* particle
*	49	* MUP4	* 0.182204E+00	* 0.136921E+02	*
*	50	* MUP5	* 0.511000E-03	* 0.511000E-03	*
*	51	* MUM1	* -.303850E+01	* 0.310788E+01	* second
*	52	* MUM2	* -.338481E+01	* 0.358694E+01	* decay

```

* 53 * MUM3 * -.135949E+02 * 0.127755E+02 * particle
* 54 * MUM4 * 0.188318E+00 * 0.136271E+02 *
* 55 * MUM5 * 0.511000E-03 * 0.511000E-03 *
* 56 * PIZ1 * 0.000000E+00 * 0.000000E+00 * third decay
* 57 * PIZ2 * 0.000000E+00 * 0.000000E+00 * particle
* 58 * PIZ3 * 0.000000E+00 * 0.000000E+00 * (“unstable”
* 59 * PIZ4 * 0.000000E+00 * 0.000000E+00 * meson:  $\pi^0$ ,  $\rho^0$ ,
* 60 * PIZ5 * 0.000000E+00 * 0.000000E+00 *  $J/\psi$ )
* 61 * PH1 * 0.000000E+00 * 0.000000E+00 * first
* 62 * PH2 * 0.000000E+00 * 0.000000E+00 * particle from
* 63 * PH3 * 0.000000E+00 * 0.000000E+00 * “unstable”
* 64 * PH4 * 0.000000E+00 * 0.000000E+00 * meson
* 65 * PH5 * 0.000000E+00 * 0.000000E+00 *
* 66 * PH01 * 0.000000E+00 * 0.000000E+00 * second
* 67 * PH02 * 0.000000E+00 * 0.000000E+00 * particle from
* 68 * PH03 * 0.000000E+00 * 0.000000E+00 * “unstable”
* 69 * PH04 * 0.000000E+00 * 0.000000E+00 * meson
* 70 * PH05 * 0.000000E+00 * 0.000000E+00 *
*****

```

E List of routines and functions

```

BREIT      non-relativistic Breit-Wigner mass distribution
DCROSS     vector product between two vectors
DEPHI     azimuthal angle determination
DIPSI     main program
DIPSIGEN  generation of kinematic variables
DIPSINI   initialisation
DIPSOUT   cross section evaluation and output
DPHELI   helicity angles determination
GLUONS    evaluation of gluon distribution
JDK       two-body decay
JPRYSKIN  cross section determination
HELOMEGA  helicity angles for three-body decays
LORENZ    three dimensional Lorentz boost
LUBEND    closing of unformatted file (lun 40)
LUBOOK    histogram and n-tuple booking
LUFIL     histogram and n-tuple filling
NTPINIT   definition of n-tuple variables
RUOTA     reference system rotation
SODING    Soeding shape distribution
SUB5      subtraction of two vectors
TIMTEM    time usage evaluation
TREDK     three-body decay (including decay of most unstable meson)

```

ULANGL angle determination
USRGLS user routine to evaluate the gluon distribution
WIGNER relativistic Breit-Wigner mass distribution

References

- [1] J.J. Sakurai, Phys. Rev. Lett. **22** (1969) 981.
- [2] For a review see e.g.
T.H. Bauer et al., Rev. Mod. Phys. **50** (1978) 261.
- [3] R.M. Egloff et al, Phys. Rev. Lett. **43** (1979) 657.
- [4] OMEGA Collab., D. Aston et al., Nucl. Phys. **B209** (1982) 56.
- [5] CHIO Collab., W.D. Shambroom et al., Phys. Rev. **D26** (1982) 1.
- [6] EMC Collab., J.J. Aubert et al., Phys. Lett. **161B** (1985) 203.
- [7] EMC Collab., J. Ashman et al., Z. Phys. **C 39** (1988) 169.
- [8] E665 Collab., M.R. Adams et al., Phys. Rev. Lett. **75** (1995) 1466.
- [9] NMC Collab., M. Arneodo et al., Nucl. Phys. **B 429** (1994) 503.
- [10] ZEUS Collab., M. Derrick et al., Z. Phys. **C 69** (1995) 39.
- [11] L. Lamberti, “Fotoproduzione esclusiva di mesoni vettori nell’esperimento ZEUS ad HERA”, Tesi di Dottorato, University of Torino (1995), unpublished (in Italian).
- [12] H1 Collab., S. Aid et al., DESY report DESY 95-251, submitted to Nucl. Phys., in print.
- [13] ZEUS Collab., M. Derrick et al., DESY report DESY 96-002, submitted to Phys. Lett. B, in print.
- [14] H1 Collab., T. Ahmed et al., Phys. Lett. **B 338** (1994) 507;
H1 Collab., S. Aid et al., DESY report DESY 96-037, submitted to Nucl. Phys.
- [15] ZEUS Collab., M. Derrick et al., Phys. Lett. **B 350** (1995) 120.
- [16] ZEUS Collab., M. Derrick et al., Phys. Lett. **B 356** (1995) 601.
- [17] H1 Collab., S. Aid et al., DESY report DESY 96-023, submitted to Nucl. Phys.
- [18] ZEUS Collab., M. Derrick et al., DESY report DESY 96-067, submitted to Phys. Lett. B, in print.

- [19] A. Donnachie and P.V. Landshoff, Phys. Lett. **B 185** (1987) 403;
 A. Donnachie and P.V. Landshoff, Nucl. Phys. **B 311** (1989) 509;
 P.V. Landshoff, Nucl. Phys. B (Proc. Suppl.) **18C** (1990) 211;
 P.V. Landshoff, in “Proceedings of the Joint LP Symposium and Europhysics Conference
 on HEP”, Geneva 1991, Editors S. Hegarty, K. Potter and E. Quercigh, World Scientific,
 Singapore, 1992, vol. 2, p. 363.
- [20] J.R. Cudell, Nucl. Phys. **B 336** (1990) 1.
- [21] M.G. Ryskin, Z. Phys. **C57** (1993) 89.
- [22] B.Z. Kopeliovich et al., Phys. Lett. **B 324** (1994) 469.
- [23] S.J. Brodsky et al., Phys. Rev. **D50** (1994) 3134.
- [24] J. Nemchik et al., Phys. Lett. **B 341** (1994) 228.
- [25] F.E. Low, Phys. Rev. **D12** (1975) 163;
 S. Nussinov, Phys. Rev. Lett. **34** (1975) 1286; Phys. Rev. **D14** (1976) 246.
- [26] V.M. Braun et al., Phys. Lett. **B 302** (1993) 291.
- [27] V.L. Chernyak and A.R. Zhitnitsky, Phys. Rep. **112** (1984) 173.
- [28] P. Söding, Phys. Lett. **19** (1966) 702.
- [29] H.J. Klein and J. Zoll, PATCHY Reference Manual, Program Library L400, CERN (1988).
- [30] CERN Program Library, CERN (1989).
- [31] R. Brun et al., FFREAD User Guide, Program Library I302, CERN (1987).
- [32] R. Brun et al., HBOOK User Guide, Program Library Y250, CERN (1992).
- [33] H. Plothow-Besch, Comp. Phys. Comm. **75** (1993) 396.
- [34] R. Brun et al., PAW, Program Library Q121, CERN (1992).
- [35] NMC Collab., M. Arneodo et al., Phys. Lett. **B 309** (1993) 222.
- [36] A. Brüll (NMC), private communication (1993).